Journal of Coastal Research	18	1	118–135	West Palm Beach, Florida	Winter 2002

Large-Scale Laboratory Measurements of Longshore Sediment Transport Under Spilling and Plunging Breakers

Ping Wang[#], Ernest R. Smith[##], and Bruce A. Ebersole[##]

[#]Department of Geology
University of South Florida
Tampa, FL 32620
U.S.A.

[##]U.S. Army Engineer
Research and Development
Center
Coastal and Hydraulic
Laboratory
3909 Halls Ferry Road
Vicksburg, MS 39180
U.S.A.

ABSTRACT

WANG, P.; SMITH E.R., and EBERSOLE, B.A., 2002. Large-scale laboratory measurements of longshore sediment transport under spilling and plunging breakers. *Journal of Coastal Research*, 18(1), 118–135. West Palm Beach (Florida), ISSN 0749-0208.

Total rates and cross-shore distribution of longshore sediment transport under predominantly spilling and plunging breakers were examined in the Large-scale Sediment Transport Facility (LSTF) at the U.S. Army Engineer Research and Development Center. The input waves were long-crested unidirectional irregular waves with broad spectra. Taking advantage of the new state-of-the-art LSTF, a suite of parameters including wave height, longshore current, longshore sediment flux, sediment concentration, and their cross-shore distribution patterns were precisely measured. The main objective of this study was to quantify the influences of different forms of wave breaking on rates and patterns of longshore sediment transport.

A significantly greater total rate of longshore sediment transport was measured under the plunging breakers than under the spilling breakers with similar breaker height. The peak longshore transport rate was measured in the swash zone for the spilling breaker case. In the case of plunging breakers, a bi-modal distribution pattern was measured with one peak in the swash zone and one in the vicinity of the breaker line. Similar rates of longshore transport were measured in the surf-bore dominated mid-surf zone for both cases. The suspended sediment concentration near the breaker line was approximately one order of magnitude greater under the plunging breakers than under the spilling breakers. Except in the inner surf zone, where faster current was measured during the plunging case, a similar cross-shore distribution of longshore current was measured for both plunging and spilling cases. Breaking type has significant influence on the magnitude and pattern of longshore transport. Parameters distinguishing dominant breaker types are important in improving the accuracy of longshore sediment transport predictions.

ADDITIONAL INDEX WORDS: *Longshore sediment transport, nearshore sediment transport, physical modeling, wave breaking, surf zone processes, sediment transport processes.*

INTRODUCTION

Accurate predictions of the total rate of longshore sediment transport and its cross-shore distribution in the surf zone are central to many coastal engineering and science studies. Present understanding and predictive tools are largely developed based on field studies (KOMAR and INMAN, 1970; INMAN *et al.*, 1981; KRAUS *et al.*, 1982; BODGE and DEAN, 1987; DEAN, 1989; SCHOONEES and THERON, 1993; WANG *et al.*, 1998a; WANG, 1998). The dynamic and non-repeatable nature of the surf zone can introduce considerable uncertainties in field measurements (WANG and KRAUS, 1999). The non-controllable nature of field conditions increases the difficulties of isolating and examining the contributions of, and interactions among, individual parameters.

In contrast to field measurements, laboratory studies have the advantages of being controllable and repeatable, allowing the isolation and examination of the contributions of individual parameters. The convenience of laboratory instrumentation enables the precise measurement of many parameters such as wave height, current, sediment concentration, and their spatial and temporal distribution patterns. The disadvantages of laboratory studies, especially the three-dimensional physical models, are their substantially reduced temporal and spatial scales and their limited capabilities of simulating real-world situations even at small scales.

KAMPHUIS (1991a, b, c) conducted a series of laboratory studies on longshore sediment transport. Irregular waves ranging from 0.05 to 0.14 m in significant wave height and 0.9 to 1.5 s (one case) in peak wave period were generated at 10 to 40 deg incident angles. Thirteen of the 21 cases, or 62%, were conducted with waves having a peak period of 1.15 s (KAMPHUIS, 1991a). There is a gap between the coverage of laboratory longshore transport measurements and field mea-

00169 received 27 December 2000; accepted in revision 20 August 2001.

surements, in terms of wave heights and periods. The smallest waves encountered in field measurements are still much higher than the highest waves in the laboratory measurements, with wave periods much longer than the 1.15 s. This gap raises the question of compatibility between field and laboratory data and predictive relations developed using the laboratory data. An overlap of wave conditions between field and laboratory data would be valuable in examining the compatibility.

In an effort to challenge the limitations of small scale and to bridge the gap between laboratory and field measurements, the U.S. Army Engineer Research and Development Center recently completed a Large-scale Sediment Transport Facility (LSTF). The LSTF is specially designed for studies of longshore sediment transport (FOWLER *et al.,* 1995). The facility has the capability of simulating wave height and period that are almost directly comparable to annual averages along many low-wave energy coasts, for example, a majority of estuary beaches (NORDSTROM, 1992), and many beaches along the Gulf of Mexico and the Great Lakes in the U.S. Detailed design considerations, capabilities, and initial testing of the LSTF are described in HAMILTON *et al.* (2001). This paper presents the results from the first phase of the LSTF study.

Based on a series of laboratory studies and re-examination of existing field data, KAMPHUIS (1991a) suggested an empirical formula for the prediction of total longshore sediment transport rate, referred to as the KAMPHUIS-91 formula in the following discussion. WANG *et al.* (1998a) found that the KAMPHUIS-91 formula predicted consistently lower total longshore transport rates than those predicted by the broadly used CERC formula (CERC, 1984) and an earlier formula suggested by KAMPHUIS *et al.* (1986), referred to as the KAMPHUIS-86 formula in the following. The lower prediction by the KAMPHUIS-91 formula, which is typically 1.5 to 3.5 times lower than predictions from the CERC and KAMPHUIS-86 formulas, occurred over a range of low wave-energy conditions with breaker height of less than 1 m (WANG *et al.,* 1998a). However, the low predictions by KAMPHUIS-91 formula matched the measured values closer than the CERC predictions for those low-wave conditions. On the other hand, MILLER (1998, 1999) found that the predictions by the CERC formula matched storm measurements with breaker height of nearly 4 m closer than the KAMPHUIS-91 predictions, which were nearly one order of magnitude lower than the measured rate.

Four types of breakers, including spilling, plunging, surging, and collapsing, have been distinguished, largely based on visual observations (PATRICK and WIEGEL, 1957; GALVIN, 1968; DEAN and DALRYMPLE, 1991; KOMAR, 1998). As summarized in KOMAR (1998), a spilling breaker gradually peaks until the crest becomes unstable and cascades down as "white water"—bubbles and foam. For a plunging breaker, the shoreward face of the wave becomes vertical, curls over, and plunges forward and downward, impinging onto part of the wave trough, with the "white water" often penetrating the entire water column and impacting the water-sediment interface directly. In surging breakers, the base of the wave surges up the beach face so that the crest collapses and disappears. Collapsing breaker is an intermediate condition between plunging and surging breakers. In general, spilling breakers tend to occur on beaches of very gentle slope with steep waves, while plunging breakers occur on steeper beaches with intermediate- to low- steepness waves. Fine-scale laboratory studies indicated that the characteristics of the turbulence generated under spilling and plunging breakers were significantly different (TING and KIRBY, 1994, 1995, 1996). Various criteria have been suggested to distinguish between the different types of breaking (*e.g.,* GALVIN, 1968; BATTJES, 1974). The criteria are typically some form of a ratio between wave steepness and beach slope. SMITH and KRAUS (1991) found that the presence of a bar could also influence the breaker type. Breaker classifications tend to describe the end-member type. In reality, there is a continuum of breaker type grading from one type to another. Also, describing the breaking processes of irregular waves is difficult. There have been studies to describe probabilities in wave breaking (THORNTON and GUZA, 1983; DALLY, 1990, 1992). These studies found that the commonly used Rayleigh distribution describes the surf zone waves, which are composed of breaking and non-breaking waves, well.

Numerous laboratory and field studies have found that suspended sediment concentrations at the breaker line are strongly influenced by breaker type (see the summary by VAN RIJN, 1993). Generally, sediment concentrations measured under plunging breakers are significantly greater than that measured under spilling breakers, given a similar breaker height (KANA, 1979; KANA and WARD, 1980; NIELSEN, 1984; VAN RIJN and KROON, 1992; VAN RIJN, 1993). Since sediment flux is the product of sediment concentration and current velocity, a different sediment concentration should result in a different rate of sediment transport given the same current velocity. Little is known about the influence of the breaker type, and hence, different sediment concentrations, on the rate and distribution pattern of longshore sediment transport.

The main objectives of this first phase of the LSTF study were to investigate and quantify the magnitude and distribution of longshore sediment transport under predominantly spilling and plunging breakers. Two long-crested unidirectional irregular wave conditions, one producing a predominantly spilling breaker and one a plunging breaker, were investigated. The input waves were generated such that a similar breaker height, but different breaker type, occurred. Wave height, longshore current, depth-integrated longshore sediment flux, vertical profile of longshore current, vertical profile of suspended sediment concentration, and the cross-shore and longshore distribution patterns of all the above parameters were measured.

METHODOLOGY AND INSTRUMENTATION

Detailed discussions on the capabilities of the LSTF, as well as the procedures of planning and executing longshore sediment transport measurements in the LSTF are discussed in HAMILTON *et al.* (2001). The LSTF has dimensions of 30-m cross-shore, 50-m longshore, and has walls 1.4 m high (Figure 1). The long-crested and unidirectional irregular waves were

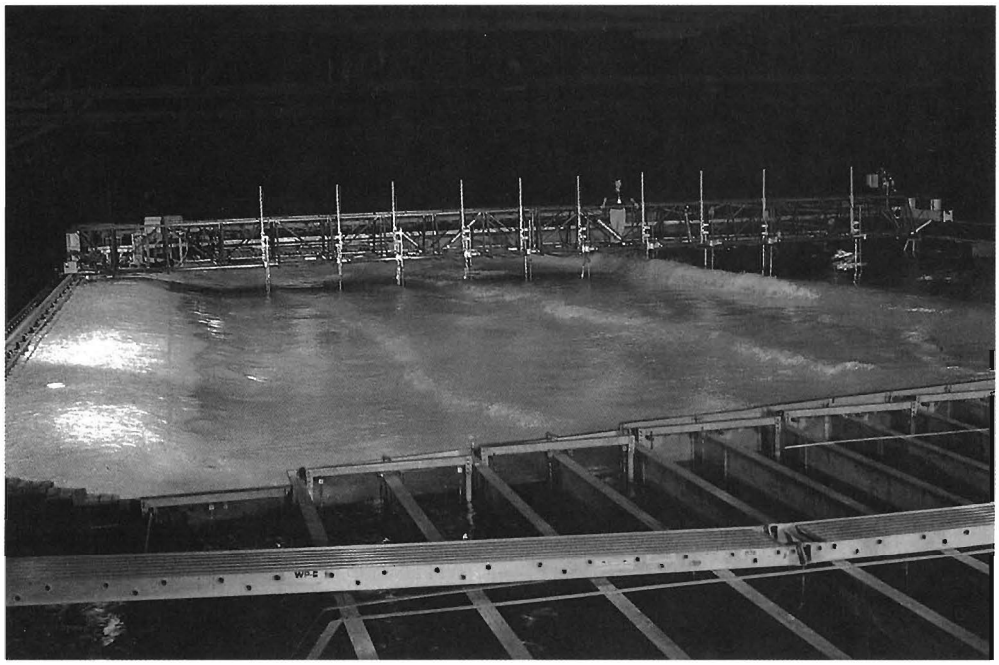

Figure 1. The LSTF during the plunging case, showing the downdrift traps in the flow channels (bottom), the instrument bridge (top), and the cross-shore array of flow meters, wave gages, and turbidity sensors.

produced by four synchronized wave generators oriented at a 10-deg angle to the shoreline. The beach was arranged in a trapezoidal plan shape corresponding to the obliquely incident waves. The beach is composed of approximately150 m^3 of very well sorted fine quartz sand with a median grain size of 0.15 mm. The sand beach was approximately 25-cm thick over the planar concrete base and extended 27 m alongshore and 18 m cross-shore, of which 15 m were below still-water level and 3 m were above. The longshore current generated by the oblique incident waves was circulated with 20 turbine pumps through 20 flow channels at the updrift and downdrift ends. The influences of the lateral boundaries can be minimized by properly circulating the wave-generated longshore current. Detailed procedures to regulate the pumps for the longshore-current circulation are discussed in HAMILTON and EBERSOLE (2001). Twenty 0.75-m wide and 6-m long bottom traps, including 18 in the flow channels (except two of the most offshore ones) and 2 landward of the shoreline, were used to measure the depth-integrated longshore sediment flux (Figure 1).

The LSTF hosts a suite of instrumentation. Details on the capabilities and accuracy of the instrument are described in HAMILTON *et al.* (2001). A brief summary of the instrumentation and sampling scheme specific to this phase of the study is listed in Table 1. The sediment-flux measurements using the downdrift bottom traps were conducted in 2 modes. Mode 1 consisted of continuous weight sampling at a frequency of 4 Hz during the wave run. Accuracy of weight measurement during the wave run was influenced by vibration and movement of the traps, which were forced by the wave motion. Mode 2 trap measurements consisted of two discrete 100-s sampling periods before and after the wave run. Accurate weights were obtained in quiescent water.

Wave height and period were measured using capacitance

Table 1. *LSTF instrumentation and sampling scheme for this study.*

Parameter To Be Measured	Instrument Type	Sampling Rate	Sampling Duration	No. Of Cross-Shore Locations	Vertical Profile
Wave	Capacitance gage	20 Hz	10 min	10#	N/A
Current	Acoustic Doppler Velocimeter (ADV)	20 Hz##	10 min	10#	Yes
Sediment concentration	Fiber Optical Backscatter (FOBS)	16 Hz	10 min	7	Yes
Water depth	Bottom-tracking profiler	every 5 mm cross-shore	between wave runs	3660	N/A
Sediment flux	Bottom sediment traps	mode 1: 4 Hz	continuous	20	No
		mode 2: 1 Hz	100 s	20	No

The 10 locations were 1.1, 27, 4.1, 5.7, 7.1, 8.5, 10.1, 11.6, 13.1, 15.6 m from the still-water shoreline, starting from ADV (or gage) #1 to ADV (or gage) #10.

The ADVs were synchronized with the wave gages.

wave gages sampling at 20 Hz. The Acoustic Doppler Velocimeters (ADVs) were used to measure current. The wave gages and current sensors were co-located in the cross-shore direction. The wave and current measurements were synchronized. The breaker angle was measured visually using the digital compass in an electronic total station transit.

Profiles of sediment concentration were measured using four arrays of the innovative Fiber Optical Backscatter (FOBS) sensors. Each array consists of 19 sensors. The vertical spacing of the sensors increased roughly exponentially upward, ranging from a 1-cm spacing in the lower portion of the array to a 6-cm spacing in the upper portion. The elevations of the FOBS sensors are controlled by referring the sensors to the bottom one, which is deployed directly on the bottom (HAMILTON *et al.,* 2001). The FOBS sensors have a high vertical resolution of 0.5 cm (MILLER, 1999). The FOBS, which were recent additions to the LSTF, were operated through a separate computer, independent of the wave-current sampling system. There was an approximately 3-s delay of the wave/current sampling relative to the sediment-concentration sampling. Improvements are currently being made to synchronize the sediment concentration and hydrodynamic measurements.

The beach profiles were surveyed using an automated bottom-tracking profiler. The beach profiles were surveyed at 1-m alongshore spacing in the middle of the test beach. A closer spacing of 0.5 m was used near the lateral boundaries to monitor the boundary influence. The profiler was programmed to sample every 0.5 cm in the cross-shore. This fine cross-shore resolution allows measurements of bed ripples.

Transport measurements for each of the wave conditions were conducted in segments. Eighteen test segments, or wave runs, of 60- to 200-minute duration were conducted for the spilling case and 13 segments of 40- to 100-minute duration were conducted for the plunging case. Each segment was designed to focus on one of the following progressive goals, with the final goal being acquisition of accurate and comprehensive measurements of the longshore sediment transport rate and its cross-shore and vertical distribution. The progressive goals listed in sequential order included:

(1) obtain optimal settings for the pump-circulation system to minimize boundary influence and circulate the longshore current;
(2) allow the beach to reach equilibrium or stable shape;
(3) provide adequate sampling coverage in the longshore and cross-shore directions;
(4) provide adequate sampling coverage throughout the water column; and
(5) repeat key measurements to ensure data quality and repeatability.

Each test segment followed the same procedure to ensure data comparability. The procedure adopted for each wave run was as follows:

(1) pre-run beach survey;
(2) pre-run trap sampling (quiescent conditions);
(3) instrument check and initialization;
(4) start sediment trap sampling;
(5) start longshore current circulation;
(6) start waves;
(7) sampling of wave, current, sediment concentration, and trap weight;
(8) stop waves;
(9) stop longshore current circulation;
(10) wash sand off the traps' rubber seals into the traps (HAMILTON *et al.,* 2001);
(11) post-run sediment trap sampling (quiescent conditions); and
(12) post-run beach survey.

Since the total amount of longshore sediment transport during individual wave runs was only a small fraction, less than 1%, of the total amount of approximately 150 m^3 of sand on the artificial beach, it was judged that continuous updrift sand recharging during the wave runs was not necessary (HAMILTON *et al.,* 2001). The beach was typically replenished after 9 hours of wave activity for the spilling case and after 3 hours for the plunging case. The wave basin was drained during this operation. The purpose of the beach replenishment was twofold, to recharge the sediment supply at the updrift end of the beach and to restore the beach to one with straight and parallel contours. The replenishment was mostly concentrated at the beach lying within 5 m from the updrift boundary. The main portion of the beach in the middle of the basin required little attention owing partly to the uniform condition maintained by the longshore current circulation system.

The principal temporal scale of this phase of the study was on the order of 10 min, representing the averages of 400 waves (at peak period) during the spilling case and 200 waves during the plunging case. It is generally accepted that averages of 150 waves or more provide reliable representation (NIELSEN, 1984; 1992). The main spatial scale was on the order of 0.75 m, or the width of the downdrift bottom traps. Parameters used in the present discussion emphasized these particular temporal and spatial scales. Processes at finer scales, such as temporal variations of currents and sediment concentrations at the dominant wave frequencies, are discussed in another paper (WANG *et al.,* in review) and are beyond the scope of this paper.

WAVE AND BEACH CONDITIONS

The Input Wave Conditions and Wave Decay in the Surf Zone

Long-crested and unidirectional irregular waves with a relatively broad spectral shape, representing typical sea conditions, were generated. The broadly-used TMA spectrum (BOUWS *et al.,* 1985) with the spectral width parameter, γ, set equal to 3.3 was used to define the incident wave spectrum. Steep waves were generated to produce predominantly spilling breakers, while low-steepness waves were generated to create predominantly plunging breakers. The significant wave height (H_{mo}) and peak wave period (T_p) were calculated using spectral analysis. A low-frequency cutoff at twice the peak wave period, 3 s for the spilling case and 6 s for the

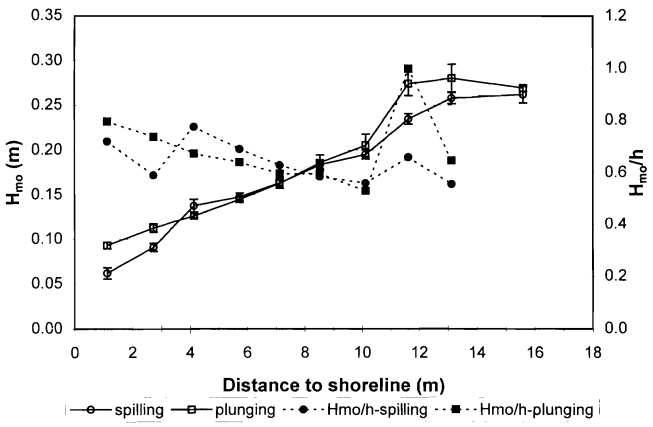

Figure 2. Patterns of the surf-zone wave decay under the spilling and plunging breakers. The error bars represent the ranges of alongshore variations.

Table 2. *Summary of wave and surf zone conditions.*

	Spilling Breaker Case	Plunging Breaker Case
Design conditions at the wave generator		
Water depth (m)	0.9	0.9
Significant wave height (m)	0.25	0.23
Peak wave period (s)	1.5	3.0
Wavelength (m)	3.4	8.7
Wave celerity (m/s)	2.2	2.9
Wave angle (deg)	10	10
Breaking wave conditions		
Significant breaker height (m)	0.26	0.27
Breaker angle (deg)	6.5	6.4
Breaking water depth (m)	0.46	0.28
Breaker index	0.57	0.96
Surf zone conditions		
Surf zone width# (m)	14.0	13.0
Surf zone slope##	1:28 (0.035)	1:43 (0.023)

The surf zone width also includes the uprush zone above the still-water shoreline.
The overall surf zone slope is calculated as the plane slope from the breaker point to the still water shoreline.

plunging case, was applied to ensure cross-shore compatibility. Energy at frequencies lower than the cutoff represented a significant contribution to the overall energy near the shoreline. This low-frequency motion, often referred to as the surf beat, might have significant influence on the modulation of sediment transport in the vicinity of the shoreline. It is beyond the scope of this paper to examine these fine-scale processes.

The main breaker-line was located at about 13.1 m from the shoreline (gage 9, 2nd from offshore) for the spilling case (Figure 2). For the plunging case, the main breaker-line was located at 11.6 m (gage 8, 3rd from offshore). Determination of the main breaker-line for irregular waves, and therefore the breaker height, was somewhat subjective. In the present study, the main breaker-line was determined to be at the location landward of which a significantly accelerated rate of wave-height decay was measured (Figure 2). This criterion was based on the comprehension that a dramatic wave-energy loss, and therefore, wave-height decrease, should follow major wave breaking. Visual observations during the wave runs supported use of this measure.

Similar significant breaker heights of 0.26 and 0.27 m were measured for the spilling and plunging cases, respectively (Table 2). About 20 breaker angles were measured during each of the segments of wave run after the beach reached a stable shape. An overall average, from all the wave runs for each wave condition, was used to represent the breaker angle. The average breaker angle for the spilling case was 6.5 deg with a standard deviation of 0.5 deg, or 8% of the mean. Similar average breaker angle of 6.4 deg with a standard deviation of 0.6 deg, or 9%, was measured for the plunging case. Except the very different forms of breaking, the present two wave cases were characterized by similar breaker height and angle.

A reasonable simplification of surf-zone longshore sediment transport is to assume that sediment is being suspended by turbulence generated by breaking waves and transported alongshore by the longshore current. Wave decay, *i.e.,* the decrease of wave height toward the shoreline, reflects the rate of wave-energy dissipation. It is often assumed that a portion of the dissipated wave energy is transferred to initiate sediment suspension. The faster the wave energy is dissipated, the more the sediment is being suspended into the water column, and hence the higher the longshore sediment flux. This approach has been adopted to model the cross-shore distribution of longshore transport (BODGE, 1986; WANG, 1998).

The significant wave heights measured at the offshore most wave gage, at about 2.5 m from the wave generators, were rather similar, 0.26 m for the spilling case and 0.27 m for the plunging case. The significant breaker height measured for the spilling case was 0.26 m, similar to the non-breaking wave height measured at the offshore wave gage. The breaker height measured for the plunging case was 0.27 m, also similar to the non-breaking wave height measured at the offshore gage. A sharp decrease of wave height was measured directly landward of the main plunging breaker line, apparently related to the dramatic wave-energy loss due to the turbulent plunging-type breaking. The wave decay following the spilling breaking was much less dramatic. Rates of wave decay in the mid-surf zone were rather similar for both the spilling and plunging cases, as indicated by the similar wave height and similar cross-shore trend of changing height (Figure 2).

Distributions of wave heights in the alongshore direction were uniform during both the spilling and plunging cases. During the spilling case, the alongshore variations, as indicated by one standard deviation, at 11 transacts were mostly within 6% of the mean except at the landward most gage, where 10% variation was measured (Figure 2). During the plunging case, the alongshore variations measured at 4 transacts were less than 7% of the mean at all the gages. Due to much more active sediment transport during the plunging case, the duration of each wave run was shorter than that of the spilling case. The shorter wave runs resulted in less

dense alongshore sampling coverage during the plunging case than during the spilling case. Maintaining satisfactory alongshore uniformity of both wave heights and longshore current velocities is essential for accurate measurement of the longshore transport rate.

The ratio of significant wave height to still water depth, the breaker index, ranged mostly from 0.6 to 0.8 (Figure 2), similar to the findings of other studies (KAMINSKY and KRAUS, 1994). A much greater value was measured at the plunging breaker line, where the ratio reached almost 1, followed by a sharp decline to slightly less than 0.6. The rapid increase of the H_{rms}/h ratio in the plunging breaker zone was caused by the sharp water-depth decrease toward the bar crest while the wave height remained nearly constant. A similar trend of landward increasing of the H_{rms}/h ratio, from slightly below 0.6 to nearly 0.8, was measured in most of the surf bore area for both the plunging and spilling cases. This suggested that the rate of wave-height decay toward the shoreline was slower than the rate of the water-depth decrease. A rapid decrease of wave height was measured near the shoreline during the spilling case, resulting in a sudden decrease of the H_{rms}/h ratio (Figure 2). The reason for this sudden wave-height decrease was not clear, and this change did not occur during the plunging-breaker case.

Beach Conditions

The 25-cm thick test beach was initially constructed based on the equilibrium shape described by BRUUN (1954) and DEAN (1977) in the form of

$$h = Ax^m \tag{1}$$

where h is the still-water depth, x is the horizontal distance from the shoreline, A is a dimensional scale parameter determined by sediment grain size, and m is the empirical shape coefficient. The m value of 2/3 was used based on DEAN (1977). For the present experiments, the A value was found to be 0.07 from the sediment grain size based on DEAN (1991). The beach profile calculated using Equation (1) was approximated with 3 planar beach segments for the convenience of construction.

The test beach was composed of very well sorted quartz sand with a median grain size of 0.15 mm. Based on HALLERMEIER (1981), the terminal settling velocity of this sand was calculated to be 1.8 cm/s. A porosity of 0.4 was used to convert between weight transport rate and volume transport rate. A relation between sediment suspension and wave orbital motion can be reflected in the commonly used DEAN number, N_o, defined as (DEAN, 1973)

$$N_o = \frac{H_o}{wT} \tag{2}$$

where w is the sediment settling velocity, T is wave period, and H_o is deep-water wave height, which can be calculated from the design wave conditions using linear wave theory. The DEAN number was found to be 10.0 and 4.4 for the spilling and plunging cases, respectively.

After a certain number of hours of wave action, the beach profile reached stable, or equilibrium, shape. The equilibrium profiles for the spilling and plunging cases are shown in Figure 3. These profiles represent averages of 16 profiles in the middle section of the test beach. In Figure 3 and the following relevant figures, the x-axis was referred to the still-water shoreline of the initial constructed beach, which was designed to be 3 m from the basin wall. Overall, alongshore-averaged shoreline changes measured during the 2 cases were small, generally less than 0.15 m. Shoreline retreat was measured during the spilling case owing to the steep erosive waves. The shoreline position was stable during the plunging case.

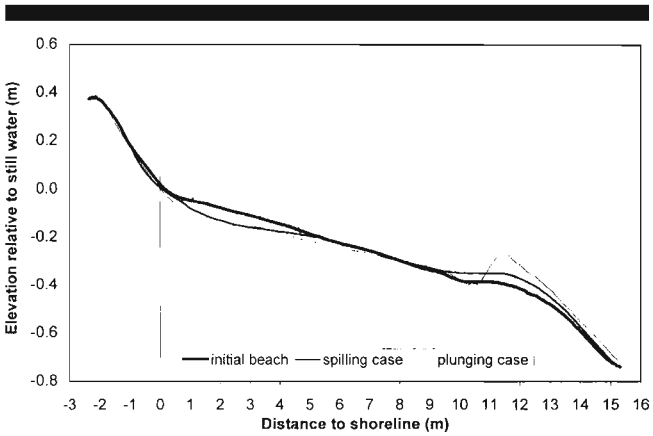

Figure 3. Equilibrium beach profiles under the spilling and plunging breakers, averages of the 16 profiles in the middle section of the test beach.

The spilling-breaker experiment was conducted with the constructed beach as the initial condition. Modest change of the beach-profile shape was measured during the spilling breaker case, as compared to the original power-function profile of Equation 1 (Figure 3). The inner surf zone was eroded and modest and broad accumulation occurred in the vicinity of the breaker line. The mid-surf zone from 5 to 9 m from the shoreline remained remarkably stable. The sand eroded from the inner surf zone was transported to and accumulated in the vicinity of the breaker line. The beach reached stable shape after 14 hours of wave action for the spilling breakers.

The plunging case was conducted using the equilibrium beach conditions generated by the spilling breakers as the initial profile. Considerable shape changes were measured for the plunging breaker case, mainly in the vicinity of the plunging point, where a substantial break-point bar developed (Figure 3). The equilibrium process took only 4 hours for the much more energetic plunging breakers. Most of the changes occurred in the vicinity of the plunging breaker line, while profile changes in other parts were relatively minor. It is beyond the scope of this paper to examine the detailed process of beach-profile evolution toward equilibrium. It was judged that the beach reached equilibrium when the apparent trend of change measured from the beginning of the wave run stopped or significantly slowed. In other words, the equilibrium beach conditions were characterized by minor trendless variations of profile shape instead of the progressive evolution toward the stable shape as observed during the early hours of wave action. The steep toe of the test beach, as lim-

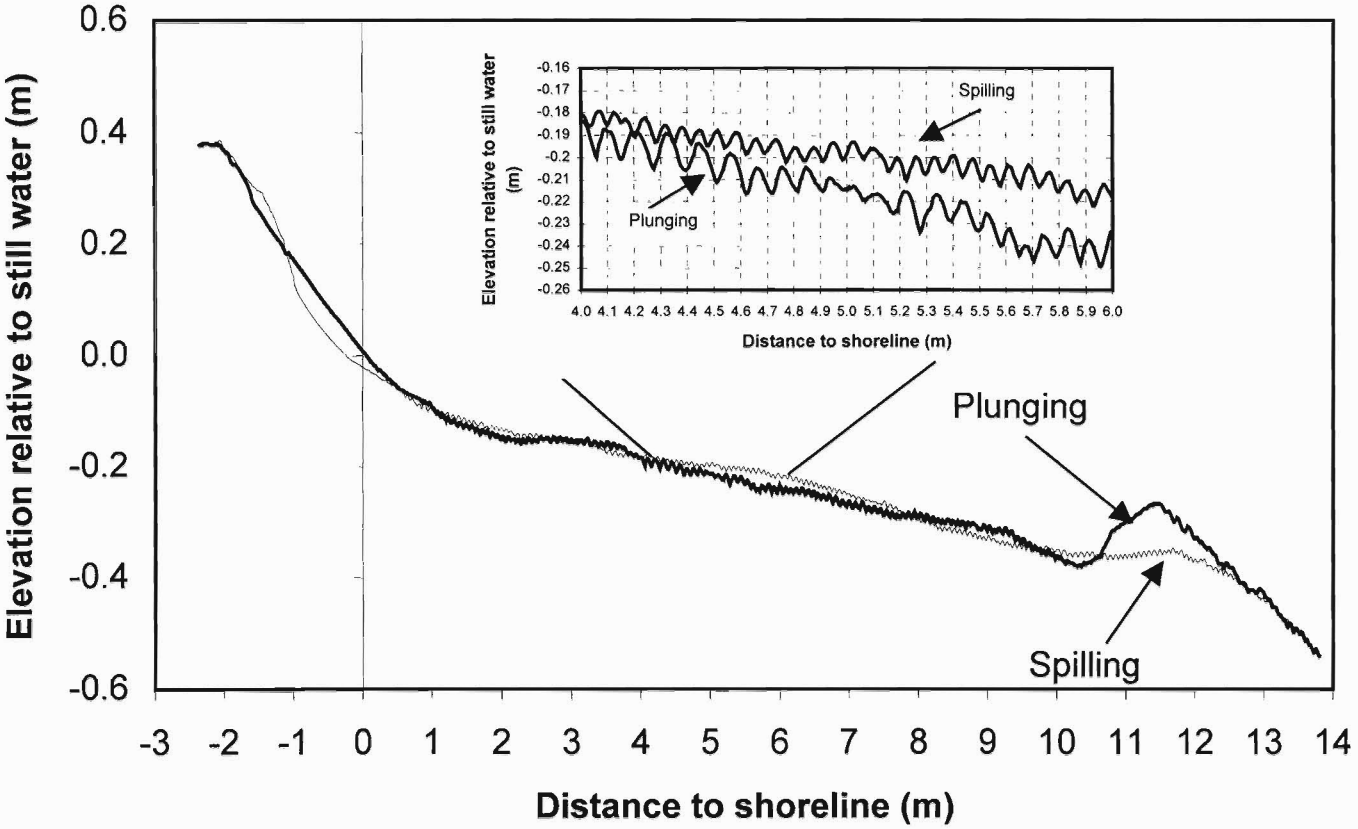

Figure 4. Examples of beach profiles showing the distribution of bed ripples and planar bed.

ited by the dimensions of the wave basin, might have some influences on wave breaking as compared to gentle beaches in the real world.

Figure 4 shows examples of individual profiles (not averaged) surveyed during the spilling and plunging experiments. Bed ripples were observed over the entire surf zone under the spilling breakers except in the vicinity of the shoreline (Figure 4). Most of the ripples were 0.7 to 1.2 cm high and 6 to 10 cm long. Under the plunging breakers, ripples were measured in the middle of the surf zone, while in the vicinity of the breaker line and shoreline, a relatively featureless bed was observed. Most of the ripples were 1.0 to 1.5 cm high and 8 to 12 cm long (Figure 4). For the convenience of discussion, the commonly used nearshore zonation is divided as follows. The swash zone ranged from the landward limit of uprush, seaward to the start of the planar bed, which roughly coincides with the seaward limit of the backwash (Figure 4). For the spilling case, the swash zone extended from 0.5 m to −0.9 m. For the plunging case, it extended from 0.9 m to −1.1 m, about 43% wider than the spilling case. The breaker zone ranged from 10 to 13 m for the plunging case and 11 to 14 m for the spilling case (Figure 4). The mid-surf zone lies between the swash and breaker zones, ranging from 0.5 to 11 m for the spilling case and 0.9 to 10 m for the plunging case. Bed ripples were largely absent in the breaker zone for the plunging breaker case. The relatively large bedforms on the seaward slope of the breakpoint bar were irregular in orientations and different from the largely shore-parallel bed ripples landward of the bar.

RESULTS AND DISCUSSION

Longshore Current

The current was measured using the array of 10 ADVs mounted at the same cross-shore locations as the wave gages (Figure 1, Table 1). The vertical current profiles were measured by positioning the sensors at different elevations in the water column (HAMILTON *et al.*, 2001). Present and previous studies in the LSTF (HAMILTON and EBERSOLE, 2001) have shown that the depth-averaged longshore current can be represented reasonably well by the velocity measured at an elevation of 1/3 water depth from the bottom. In the following discussion, the depth-averaged velocity is represented by a point measurement at this elevation in the water column.

Vertical Profile of Longshore Current

The vertical current profile was measured by positioning the sensor at a different water level during each 10-min sampling event. Therefore, a time difference of approximately 15 min (10 min for sampling and 5 min for positioning the bridge and sensors) exists among the vertical measurements. Given

that the wave and beach conditions remained largely constant through the wave runs, especially after the beach profile reached equilibrium, this time delay should not induce any significant uncertainties in the measurement of current profiles. Details on the measurement of velocity profiles are discussed in HAMILTON and EBERSOLE (2001) and HAMILTON *et al.* (2001). The present discussion is focused on time-averaged values over the 10-minute sampling interval.

Due to the lack of both field and laboratory data, relatively little is known about the longshore-current profile throughout the water column, especially near the bottom. Based mainly on mathematical derivation and verified with limited laboratory data, DEIGAARD *et al.* (1986) suggested that surf zone longshore current is relatively uniform throughout the water column except in the immediate vicinity of the bottom. SVENDSEN and LORENZ (1989) determined analytical expressions for vertical varying longshore current for a long straight coast. Longshore-current profiles measured in the LSTF over a fixed concrete bed confirmed a homogeneous profile over much of the water column (HAMILTON and EBERSOLE, 2001).

The overall shape of the longshore-current profile measured over the movable fine sand bed was not homogeneous as derived mathematically and measured over the fixed concrete bed. Logarithmic longshore-current profiles, with increasing velocity with increasing elevation from the bed, were measured at all the cross-shore locations under both the spilling and plunging breakers (Figure 5). The shape and magnitude of the longshore current profile were rather similar under both the spilling and plunging breakers. This seems to indicate that the breaker types do not have significant influence on the vertical longshore current structure in the surf zone. The similar longshore current was probably controlled by similar breaker height and breaker angle (Table 2). The bottom boundary layer over the movable bed with bed forms (except at the plunging breaker line) should be thicker than that over the relatively smooth concrete bed. This might contribute to the upward increasing velocity profile.

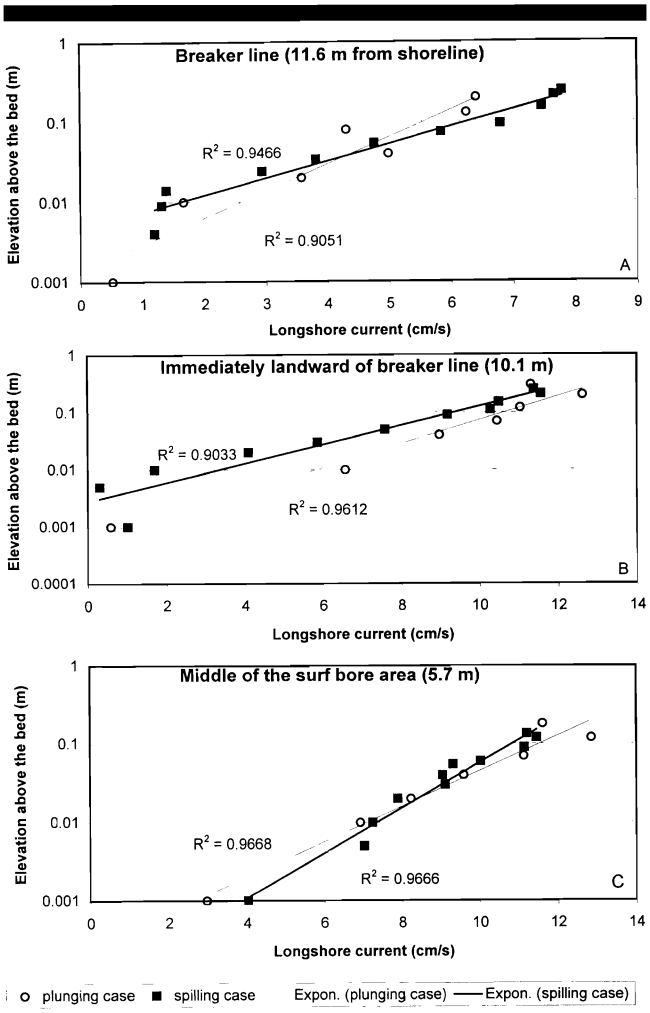

Figure 5. Time-averaged longshore current profiles at various cross-shore locations under the plunging and spilling breakers.

Alongshore Uniformity of Longshore Current

As discussed in VISSER (1991) and HAMILTON and EBERSOLE (2001), maintaining alongshore uniformity of the longshore current is critical in minimizing the boundary disturbance and producing the most accurate measurement of longshore transport rate. It was necessary to accurately circulate the wave-generated longshore current with pumps to maintain longshore uniformity. Detailed procedures for examining the degree of longshore uniformity in longshore currents are discussed in HAMILTON and EBERSOLE (2001). After a series of iterations, a reasonably uniform longshore current pattern was achieved. The magnitudes and cross-shore distribution of longshore-current velocity measured at different alongshore locations over the middle 15-m test section of the wave basin were rather similar (Figure 6), indicating a uniform condition alongshore. Throughout most of the surf zone, the longshore currents generated by the circulation pumps are in good agreement with currents generated by the oblique incident waves (Figure 6).

Cross-Shore Distribution of Longshore Current

Because the suspended sediment is transported alongshore by the longshore current, the cross-shore distribution of longshore current has a significant influence on the patterns of longshore sediment transport. The cross-shore distribution of longshore current for both the spilling and plunging cases are illustrated together in Figure 7. The cross-shore pattern plotted in Figure 7 represents the average of measurements from the alongshore transacts shown in Figure 6.

Slightly greater longshore current was measured in the breaker zone from 10 to 13 m for the plunging case than the spilling case (Figure 7). At the main spilling breaker line at around 13 m, the longshore current was relatively weak. A rapid increase was measured immediately landward of the breaker line. A weak longshore return current (toward the updrift end of the facility) was measured at the seawardmost ADV, indicating some re-circulation in the basin. HAMILTON and EBERSOLE (2001) discussed in detail the procedures of minimizing the return flow via optimal pump settings. The longshore current in most of the surf-bore area remained

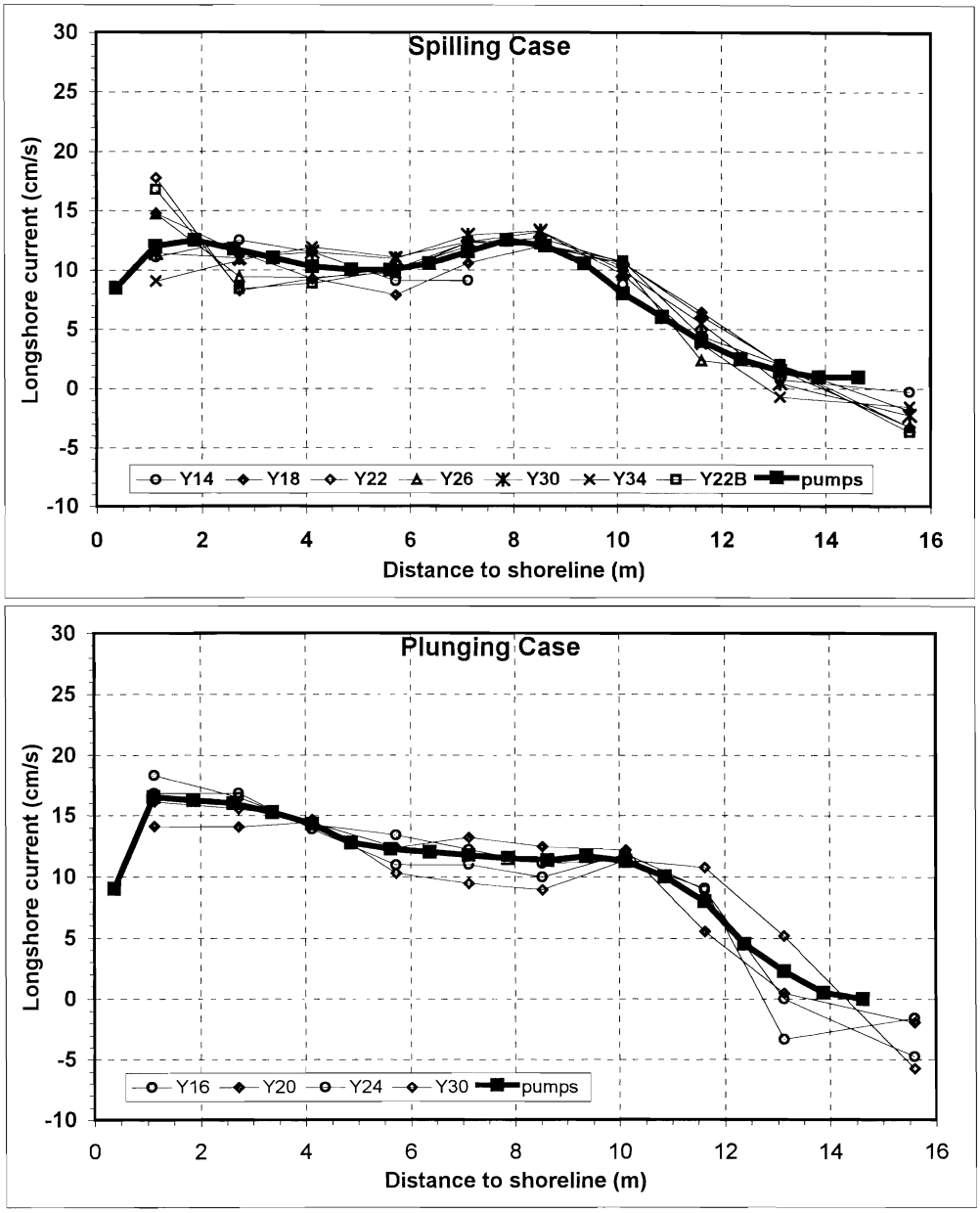

Figure 6. Alongshore uniformity of longshore current and the rates of pump circulation, legend numbers indicate alongshore locations in meters.

rather constant at about 10 to 12 cm/s during both spilling and plunging cases.

Two subtle peaks were measured during both the spilling and plunging cases (Figure 7). For the spilling case, one peak was measured just landward of the breaker zone and one just seaward of the swash zone. For the plunging case, the seaward peak was located slightly seaward of the peak for the spilling case and was inside the presently defined breaker zone. Bi-model or broad cross-shore distribution patterns of longshore current have been measured in the field by KRAUS and SASAKI (1979) and SMITH *et al.* (1993). These patterns are quite different from the predictions from the simple analytical model of LONGUET-HIGGINS (1970) for regular waves, which predicts the peak longshore current just landward of the breaker line over a plane beach. Some recent numerical models such as those of KRAUS and LARSON (1991), SMITH *et al.* (1993), SLINN *et al.* (2000) are capable of incorporating more complicated bottom profile and reproducing more complicated distribution patterns. Due to the shallow and 100% variation of water depth in the swash zone, current velocities could not be measured in this zone. However, dye observations indicated strong longshore current, which was comparable to that measured at the landward most current meter.

Overall, the differences in magnitudes and patterns of

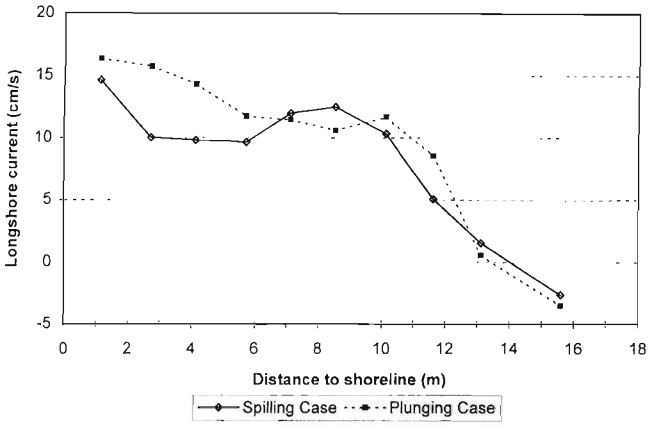

Figure 7. Cross-shore distribution of longshore current under the spilling and plunging breakers.

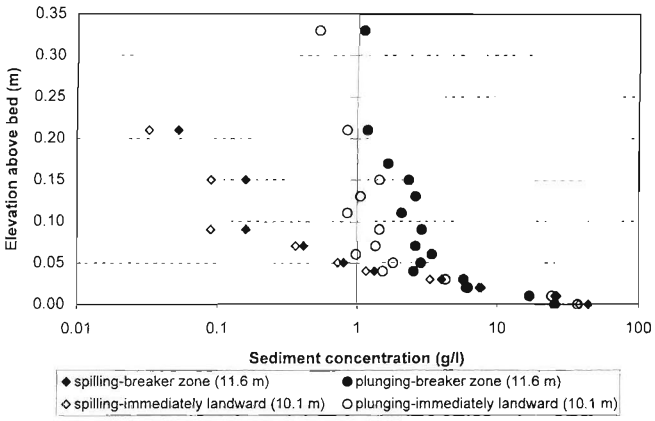

Figure 8. Suspended sediment concentration in the breaker zone. Numbers in the legends denote distance to the still-water shoreline.

longshore current between the spilling and plunging cases were relatively minor. These, together with the similar longshore-current profiles throughout most of the surf zone (Figure 5), indicate that different breaker types did not significantly change the characteristics of longshore current. The similar breaking wave height, angle, and wave-decay patterns may be the dominant factors. Under both cases, peak longshore current was measured at the landward-most gage just seaward of the swash zone. The reason for the slightly greater longshore current measured near the shoreline during the plunging case than during the spilling case was not clear. The swash zone, *i.e.,* the zone of up- and down-rushing, was wider during the plunging case.

Suspended Sediment Concentration

For the convenience of discussion, the suspended sediment is defined here as all the particles that are in motion above the bed level, regardless of whether or not the sediment is in frequent contact with the bed. This should not be confused with the commonly used concepts of bedload and suspended load, which are theoretically distinguished based on the frequency of the particles' contact with the bed. The concepts of bedload and suspended load are helpful in understanding the modes of sediment movement. Practically, they cannot be measured separately. The suspended sediment referred to here should contain the entire suspended-load and the portion of the bed-load that was not rolling on the sediment surface. The following discussion is focused on the characteristics of the time-averaged sediment concentration over the 10-min sampling interval.

The overall magnitudes and shapes of the suspended sediment concentration profile are significantly different in the breaker zone for the spilling and plunging cases (Figure 8). Similar suspended sediment concentrations were measured within 3 cm from the bed during both the spilling and plunging cases. Above 5 cm from the bed, the suspended sediment concentration in the breaker zone was more than one order of magnitude greater during the plunging case than during the spilling case. Under the plunging breakers, the sediment concentration remained fairly constant throughout the water column from 5 cm to nearly 35 cm above the bed, ranging from 1 to 3 g/l. This seems to indicate that the strong turbulent mixing under the plunging breakers dominated the settling of the fine sand particles. This nearly homogeneous sediment suspension was not measured under the spilling breakers. The rapidly decreasing concentration with elevation above the bed indicates that vertical mixing under the spilling breakers was not strong enough to suspend significant amounts of sediment high into the water column.

The similar sediment concentrations measured within 3 cm from the bed at the spilling and plunging breaker line were puzzling, given the very different hydrodynamic and bottom conditions. Almost identical near-bed sediment concentrations were also measured by NIELSEN (1979), and summarized in NIELSEN (1992, p. 219), for non-breaking waves and spilling breakers. A conclusion was drawn that except for extreme case of plunging jet hitting the bed, the pickup rate at the bed and hence the near-bed sediment concentration was not affected by the spilling breaking. NIELSEN (1992) further concluded that the main effect of the turbulence from wave breaking is a vertical stretching of the concentration profile, i.e., much greater concentration high in the water column. Our data from the LSTF indicated that even when the plunging jet was hitting the bed, the near-bed sediment concentrations were still remarkably similar. Almost identical near-bed concentrations were also measured by BOSMAN (1982), and summarized in VAN RIJN (1993, p. 8.18–8.19), under non-breaking waves, spilling breakers, and plunging breakers. BOSMAN (1982) used direct pump-suction samplers over a flat bed in the vicinity of the breaker line. No interpretation for the "approximately constant" near-bed concentrations was provided.

The shapes of the suspended sediment concentration profiles in the mid-surf zone, from about 1 to 9 m from the still-water shoreline, were similar during the plunging and spilling cases (Figure 9). A slightly greater sediment concentration was measured during the spilling case than during the plunging case. This is consistent with the similar wave con-

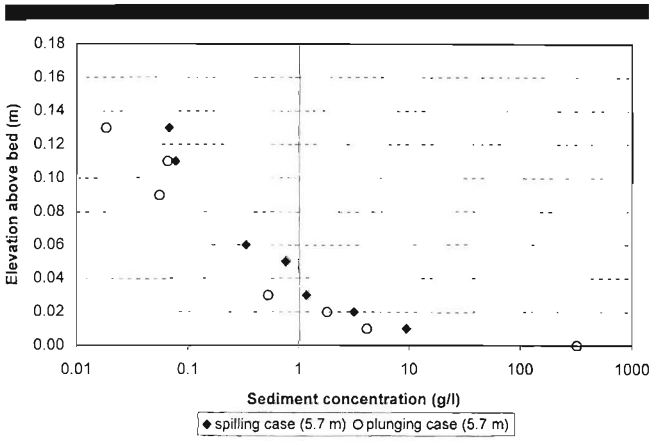

Figure 9. Suspended sediment concentration in the mid-surf zone, an example at 5.7 m from shoreline.

ditions measured in the surf-bore area (Figure 4). This also indicates that the cross-shore mixing of the active sediment suspension from the plunging breaker line at about 12 m was limited to the narrow breaker zone between 10 to 13 m and did not have significant influences on concentrations in most of the mid-surf zone. The suspended sediment concentration decreased rapidly with increasing elevation from the bed, indicating limited vertical mixing under the surf bore.

Active sediment movement was observed in the swash zone, mostly in a sheet flow mode, as reflected by the planar bed. The turbidity sensors could not function properly in the very shallow water with depth variation of 100%. Overall, the influences of breaker types on sediment suspension were limited in the vicinity of the breaker line. Lateral mixing did not seem to play a significant role in sediment suspension throughout the entire surf zone.

Sediment Flux

Depth-integrated longshore sediment flux was measured by the 20 bottom traps at the downdrift end of the wave basin. The traps are 0.75 m wide and provide precise measurements of the total sediment flux across this width. A disadvantage of the bottom traps is that they cannot provide information on the vertical distribution of the longshore sediment flux through the water column.

Sediment flux can also be calculated from the sediment concentration and current measurements. By definition, sediment flux, $F(x, z, t)$, is the product of sediment concentration, $c(x, z, t)$, and particle velocity $v(x, z, t)$,

$$F(x, z, t), = c(x, z, t), \times v(x, z, t), \quad (3)$$

where t is time, and x and z are cross-shore and vertical coordinates, respectively. Because the sediment concentration and current measurements were not exactly synchronized, the instantaneous sediment flux could not be calculated from Equation 3. In the following, $v(x, z)$ and $c(x, z)$ values averaged over the 10-min sampling interval were used to estimate a time-averaged sediment flux. This simplification is acceptable if either longshore current or sediment concentration is reasonably steady over time. Sediment concentration varied greatly with time, dominated by the sediment suspension events that typically followed the breaking of high waves. Detailed temporal variations of sediment concentration and current and their relations are discussed in WANG *et al.* (in review).

Figure 10 illustrates two examples of the temporal variations of longshore current. For the spilling case (Figure 10, upper panel), the standard deviation of the temporal average of the longshore current velocity was 4.9 cm/s, or about 38% of the mean. A slightly greater variation of 54% of the mean was measured during the plunging case (Figure 10, lower panel). In addition to this reasonably steady longshore current, WANG *et al.* (in review) found that the temporal variations of longshore current and sediment concentration seemed to be random relative to each other without any regular phase-angle difference. Based on the above analyses, WANG (*et al.*, in review) suggested that the product of time-averaged sediment concentration and longshore current should provide a reasonable estimate of longshore sediment flux.

Vertical Distribution of Sediment Flux

The vertical profiles of sediment flux discussed in this section were calculated based on Equation 3 using time-averaged sediment concentration and longshore current. Realizing that the neglected contributions from time-variant portions could not be quantified, the present discussion focuses on the trends of the profiles and comparative magnitudes. Precise depth-integrated sediment flux, or the total sediment transport rate per unit width, was measured at the downdrift bottom traps. Within 3 cm from the bed the measurements of sediment concentration and longshore current were conducted at the same levels, at 1-cm intervals. Minor differences (typically less than 3 cm) in measurement levels existed in the upper portion of the water column. Since the vertical gradient of sediment concentration was much greater than that of the longshore current, the longshore current was linearly interpolated to match the levels of the sediment concentration measurements.

In the breaker zone, the longshore sediment flux above 5 cm from the bed was approximately one order of magnitude greater during the plunging case than during the spilling case (Figure 11). This was controlled by the much greater sediment concentration (Figure 8), because the longshore-current profiles were similar (Figures 5 and 7). The longshore sediment-flux profile under the plunging breakers was fairly homogeneous throughout the water column above 5 cm from the bed. The relatively mild upward-decreasing sediment concentration was compensated by the upward-increasing longshore current. Under the spilling breakers, sediment flux decreased with distance above the bed, dominated by the rapid upward-decreasing sediment concentration. Under the plunging breakers, the longshore sediment flux throughout the entire water column at the breaker line (at 11.6 m from the shoreline) was consistently less than the flux immediately landward (at 10.1 m). This was because the longshore current

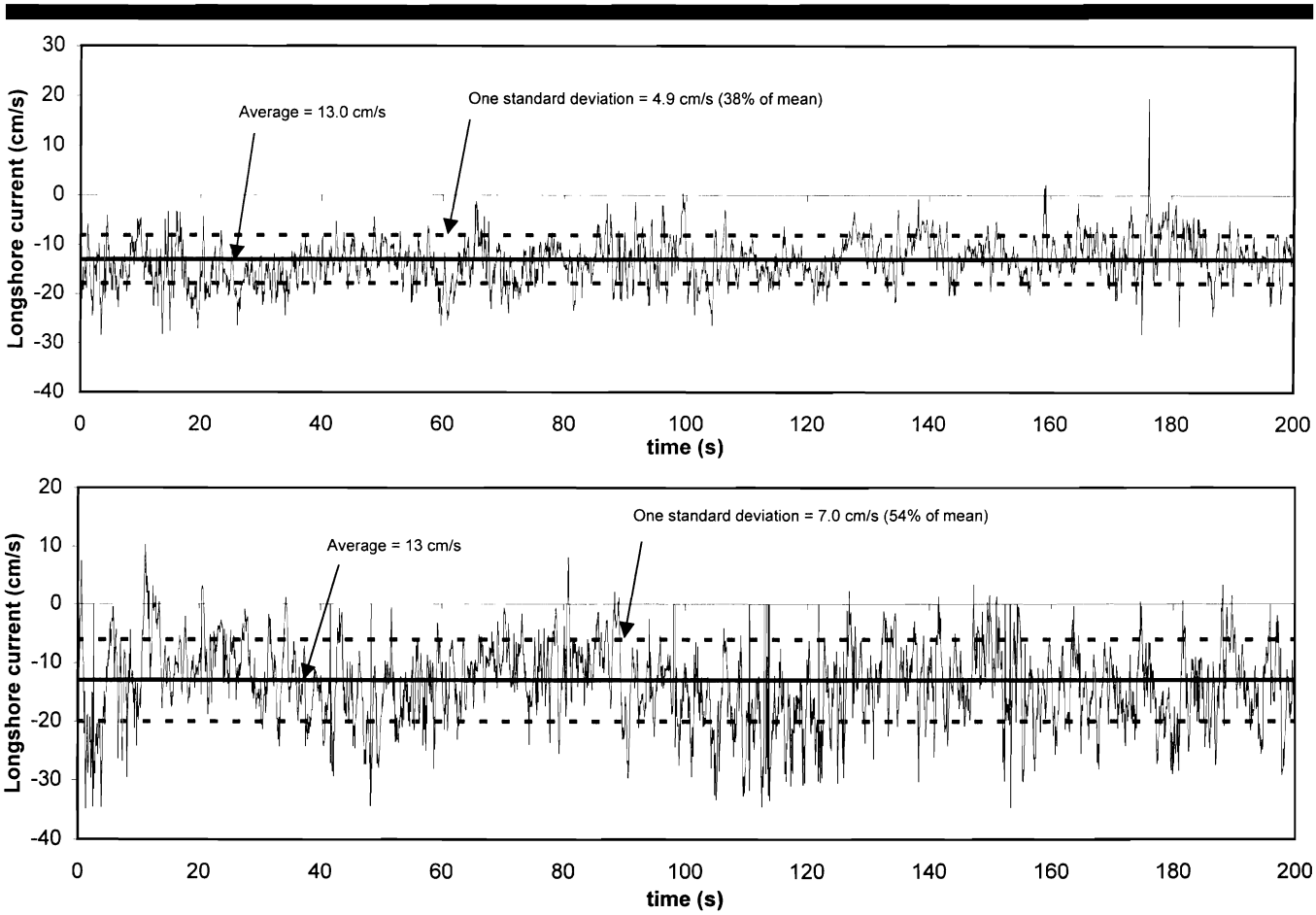

Figure 10. Steadiness of longshore current, 200-s segments of the 600-s recording are shown. Upper: spilling case at 8.5 from shoreline; lower: plunging case at 8.5 m from shoreline.

at the breaker line was smaller than that immediately landward (Figure 7).

In the mid-surf zone, slightly greater sediment flux was measured during the spilling breaker case than during the plunging breaker case (Figure 12). This was caused by the slightly greater suspended sediment concentration measured in the surf-bore area during the spilling case (Figure 9). Except in the vicinity of the plunging breaker line, the majority of sediment transport occurred close to the bed. This is because the sediment concentration was one or two orders of magnitude greater near the bed, overcoming the weaker near-bottom longshore current. For the present 2 cases, over 75% of the total longshore sediment flux occurred within 5 cm from the bed in the mid-surf zone. However, at the plunging breaker line at 11.6 m, only 29% of the total longshore flux occurred within 5 cm from the bed, and over 70% of the longshore flux occurred high in the water column. The near-bed longshore flux increased to 46% of the total immediately landward of the plunging breaker line at 10.1 m from shoreline. At the spilling breaker line, 73% of the total longshore flux occurred within 5 cm from the bed, similar to the surf-bore area.

Cross-Shore Distribution of Longshore Sediment Flux

The depth-integrated longshore sediment flux over a 0.75-m cross-shore section of the beach measured at the downdrift traps is used here to discuss the cross-shore distribution patterns. The trap measurements are direct and accurate. The cross-shore distribution patterns of the depth-integrated longshore sediment flux were quite different during the plunging and spilling cases (Figure 13). The cross-shore distribution of longshore sediment transport was far from being uniform. For the spilling case, the peak longshore transport was measured in the swash zone. Two transport peaks, one in the swash zone and one in the breaker zone, were measured during the plunging case.

For both cases, significant sediment transport was measured in the swash zone. The swash zone is characterized by a planar bed regime, as compared to the rippled surf-bore area (Figure 4). The planar bed was apparently generated by the extremely active interaction between the up- and downrush and the bottom sediment. For the spilling case, about 27% of the total longshore sediment transport occurred in the

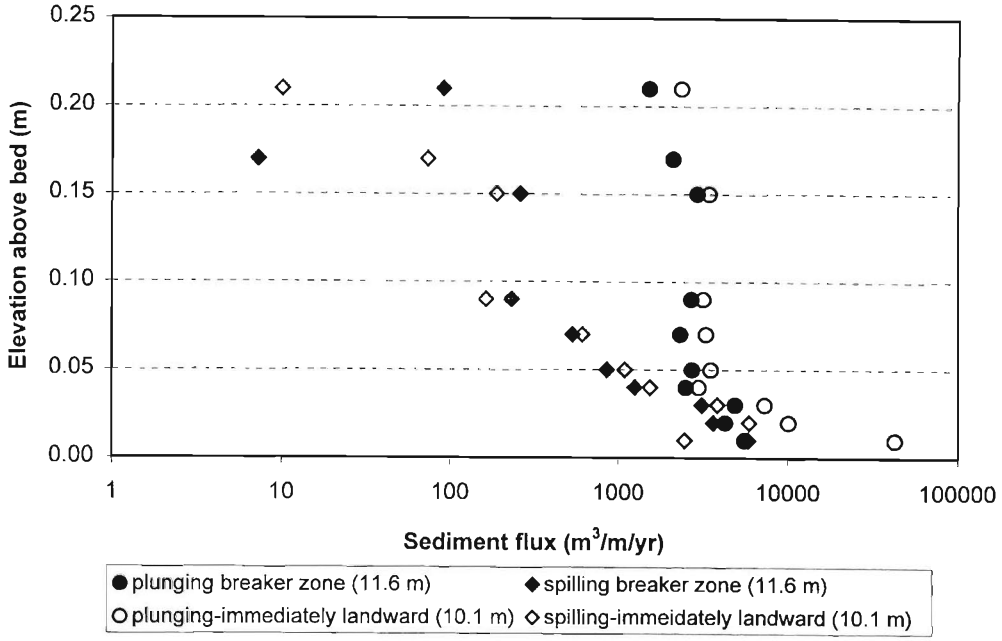

Figure 11. Sediment-flux profiles in the breaker zone. Numbers in the legends denote distance to the still-water shoreline.

narrow swash zone (Figure 13). The 1.4-m (0.5 to −0.9 m) width of the swash zone was approximately 10% of the total surf-zone width of 14.0 m (including 0.9 m landward of the still-water shoreline reached by the uprush). For the plunging case, about 34% of the total longshore sediment transport occurred in the swash zone, which was approximately 15% (0.9 to −1.1 m) of the total surf-zone width of 13.1 m (including 1.1 m landward of the still-water shoreline reached by the uprush). A substantial amount of longshore sediment transport occurred landward of the still-water shoreline, especially during the plunging case. The peak longshore flux was measured in the trap just landward of the still-water

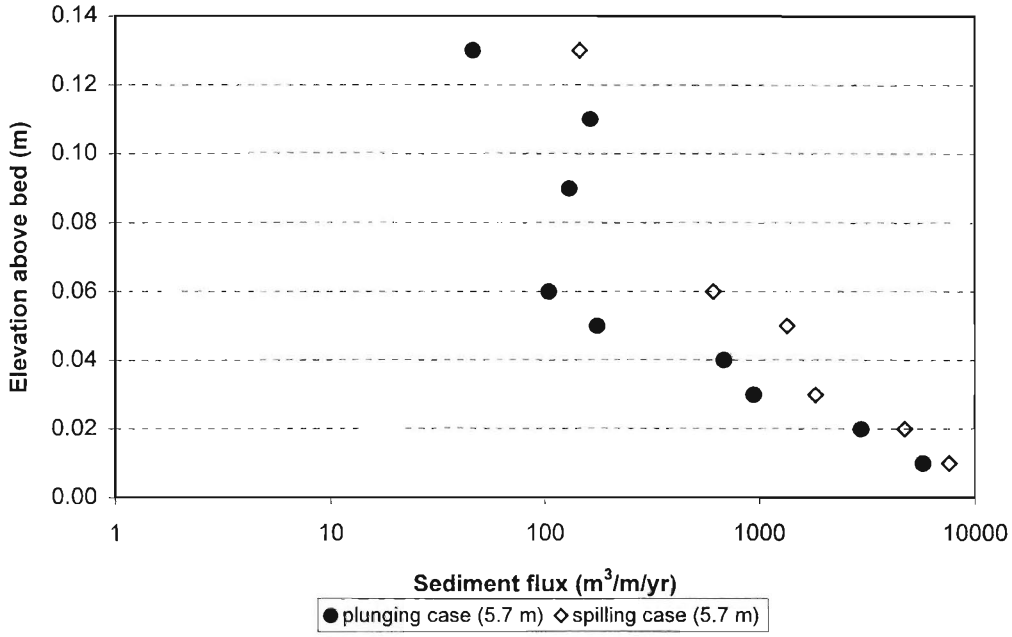

Figure 12. Sediment-flux profiles in the mid-surf zone. Numbers in the legends denote distance to the still-water shoreline.

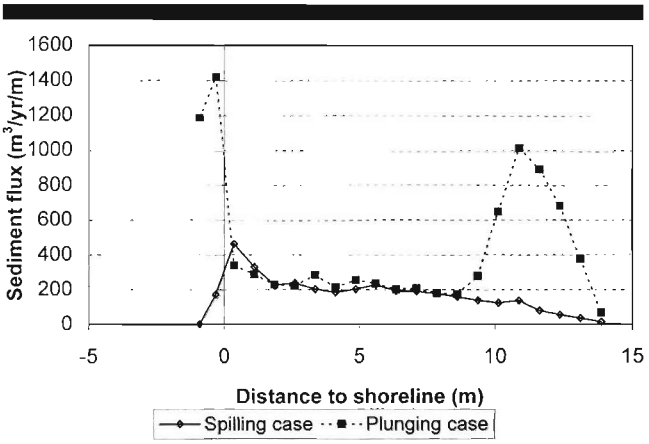

Figure 13. Cross-shore distribution of longshore sediment transport under the spilling and plunging breakers.

shoreline (Figure 13). Nearly 28% of the total longshore sediment transport occurred landward of the still-water shoreline during the plunging case. During the spilling case, less than 5% of the total transport was trapped landward of the still-water shoreline. Visual observations during the experiments indicated that the uprush was much more active during the long-period plunging case than that during the spilling case. This was probably responsible for the much greater sediment flux above the still-water shoreline.

Active sediment transport in the swash zone was also observed in several field and laboratory studies (KRAUS *et al.*, 1982; BODGE and DEAN, 1987; KRAUS and DEAN, 1987; KAMPHUIS, 1991a; WANG, 1998). Instantaneous sediment concentrations of up to 110 g/l, far greater than that in any other portions of the surf zone, have been measured by ZAMPOL and INMAN (1989) in the swash zone. The swash zone usually has the coarsest sediment as compared to that on the dry beach and in other parts of the surf zone (DAVIS *et al.*, 2000). One explanation of the coarse swash zone sediment is that fine grains are being moved away by the active transport leaving the relatively coarse sediment on the bed (WANG *et al.*, 1998b). Little is known about quantitative swash zone processes. The main obstacle is the technical difficulty of conducting accurate measurements in this dynamic narrow zone with 100% variation of water depth. This is an area of continued research at the LSTF.

A substantial and relatively broad peak of longshore sediment flux was measured in the vicinity of the plunging breaker line (Figure 13). This peak was related to the active sediment suspension throughout the entire water column induced by the turbulent plunging-type breaking. Nearly 35% of the total longshore sediment transport occurred in the 3-m wide breaker zone from 10 to 13 m. This zone represented 23% of the total surf-zone width of 13.1 m. Combined with the swash-zone peak, nearly 70% of the total longshore transport occurred in the breaker and swash zones. These two areas together occupied less than 40% of the total surf zone width. Active sediment suspension and transport in these two zones are also indicated by the planar bed regime. In the swash zone, the planar bed was caused by active sheet flow motion. At the plunging breaker line, the planar bed seemed to be induced by a combination of the sheet flow and strong turbulence, which also resulted in active sediment suspension high into the water column. No transport peak was measured at the spilling breaker line.

Similar magnitude and distribution pattern of the longshore sediment flux were measured in the mid-surf zone for both the spilling and plunging cases (Figure 13). The similar sediment fluxes are consistent with the similar distribution patterns of wave height and decay (Figure 2) and longshore current (Figure 7) in the mid-surf zone. These indicate that the breaker types did not have significant influence on the surf bore dynamics in the mid-surf zone. A gradual trend of increasing sediment flux toward the shoreline was measured. According to the energy-dissipation model of DALLY *et al.* (1985), an increasing ratio of breaker height to water depth (Figure 4) would result in an increased rate of energy dissipation, which could contribute to the increasing magnitude of longshore sediment flux toward the shoreline. The dynamics and energy dissipation of spilling breakers and surf bores are described reasonably well by the surface roller theory (SVENDSEN, 1984a, 1984b). Both these models were developed based on the understanding of the spilling type of breaking. Considerable modifications may be necessary to adopt these models to describe plunging breakers.

Total Rate of Surf-Zone Longshore Sediment Transport

The total rate of longshore sediment transport in the surf zone is an important and commonly used parameter in coastal research and engineering projects. One of the goals of the LSTF is to improve the accuracy of predictions of the total rate of longshore transport (FOWLER *et al.*, 1995). A commonly used tool for predicting the total rate of longshore transport is the CERC formula (CERC, 1984)

$$I_l = \frac{K_l}{16\sqrt{\gamma}}\rho g^{3/2} H_{sb}^{5/2}\sin(2\theta_b) \tag{4}$$

where I_l is the submerged-weight transport rate, γ is the breaker index, often taken to be 0.78, ρ is the density of the water, g is gravitational acceleration, H_{sb} is significant breaking wave height, θ_b is wave breaker angle, and K_l is an empirical coefficient. Based on the original field study by KOMAR and INMAN (1970), the Shore Protection Manual (CERC, 1984) recommended a K_l value of 0.39. BODGE and KRAUS (1991) re-examined the derivation and suggested a lower K_l value of 0.32. SCHOONEES and THERON (1993, 1994) re-examined the 46 most reliable of the 240 existing field measurements that have been compiled to determine a K_l value of approximately 0.41. The physical foundation of the CERC formula is that the rate of sediment transport is proportional to a measure of the wave-energy flux.

Based on similar field data, KAMPHUIS *et al.* (1986) developed an empirical formula, which includes the beach slope and sediment grain size

$$Q = 1.28\frac{H_{sb}^{3.5} m}{d}\sin(2\theta_b) \tag{5}$$

where d is sediment grain size, and m is beach slope. With additional laboratory study and further analysis of the existing field data, KAMPHUIS (1991a) modified the 1986 formula, adding the influence of peak wave period, T_p

$$Q = 6.4 \times 10^4 H_{sb}^2 T_p^{1.5} m^{0.75} d^{-0.25} \sin^{0.6}(2\theta_b) \quad (6)$$

The Q in Equation 6 is the total volume transport rate in the units of m^3/yr. It is noted that the dependence on grain size and wave height were greatly reduced in the newer Equations 6 as compared to Equation 5. The influences of beach slope and incident wave angle were also reduced. The coefficients in the above forms of KAMPHUIS-86 and −91 formulas were determined using metric units.

KRAUS *et al.* (1988) adopted a different approach as compared to those above, which assume a proportionality between longshore transport rate and longshore wave-energy flux. KRAUS *et al.* (1988) assume that the total rate of longshore sediment transport in the surf zone is proportional to the longshore discharge of water:

$$Q \propto K_d(R - R_c) \quad (7)$$

where K_d is an empirical coefficient that may relate to sediment suspension, R_c is a threshold value for significant longshore sand transport, and R is called the discharge parameter and is proportional to the average discharge of water moving alongshore. In the LSTF, R is accurately measured. In the field, R can be calculated as

$$R = nV_{ls}x_bH_b \quad (8)$$

where n is a constant, V_{ls} is the average longshore current velocity, x_b is the surf-zone width, and H_b is the breaker height. Based on field data collected using streamer sediment traps at Duck, North Carolina, KRAUS *et al.* (1988) suggested a K_d value of 2.7 and R_c value of 3.9 m^3/s.

In the LSTF, the total rate of longshore sediment transport was obtained by simply summing the sediment flux measured at all the traps. The total rate measured during the spilling case was 2,660 m^3/yr, substantially less than the total rate of 7,040 m^3/yr measured during the plunging case. The breaking wave was about 4% higher during the plunging case, 0.27 m versus 0.26 m during the spilling case (Table 2). Despite the slightly lower waves generated at the wave board, the more significant shoaling of the long-period waves resulted in slightly higher breakers. The 4% higher breaker could not explain the fact that measured total longshore sediment transport rates differed by a factor of 2.65. The much more active sediment suspension under the plunging breakers and the greater transport in the wider swash zone apparently contributed to the greater rate of total transport.

The measured total transport rates were substantially lower than the predictions from the CERC formula (Equation 4) and the KAMPHUIS-86 formula (Equation 5) for both the spilling and plunging cases (Table 3). The KAMPHUIS-91 (Equation 6) formula, on the other hand, under-predicted the measured rates for both cases. The empirical K_l value of 0.39 as recommended by the *Shore Protection Manual* (CERC, 1984) was used in Equation 4.

The CERC formula over-predicted the total rate for the spilling condition by over 700%, while for the plunging breakers; the over-prediction was less than 250%. This inconsistency of the CERC formula under different breaker types indicates that a simple reduction (or increase) of the K_l value as examined by BODGE and KRAUS (1991), SCHOONEES and THERON (1993, 1994), and WANG *et al.* (1998a) cannot completely solve the problem. In other words, the comprehension that the total rate of longshore sediment transport is proportional to a measure of the longshore wave-energy flux at the main breaker line might not be complete. The KAMPHUIS-86 formula also had a similar inconsistency. The spilling case was over-predicted by more than 300%, while the plunging case was over-predicted by less than 30%.

Table 3. *Comparison among measured and predicted total rate of longshore sediment transport.*

	Spilling Case	Plunging Case
TRANSPORT RATES (m^3/yr)		
Measured (m^3/yr)	2,660	7,040
CERC formula (m^3/yr)	22,030	23,850
KAMPHUIS-86 (m^3/yr)	10,760	9,100
KAMPHUIS-91 m^3/yr)	2,200	5,360
KRAUS-88 (m^3/yr)	2,670	3,150
RATIOS OF PREDICTED VERSUS MEASURED		
CERC/measured	8.28	3.39
KAMPHUIS-86/measured	4.05	1.29
KAMPHUIS-91/measured	0.83	0.76
KRAUS-88/measured	1.00	0.45
PERCENTAGE OVER (+) OR UNDER (−) PREDICTION		
CERC	+728%	+239%
KAMPHUIS-86	+305%	+29%
KAMPHUIS-91	−17%	−24%
KRAUS-88	0%	−55%

By incorporating wave period to a power of 1.5, the KAMPHUIS-91 formula produced more consistent predictions for the different breaker types, as compared to the measured values. Wave period, which is linked to the wavelength through the dispersion relation, has significant influence on wave steepness and hence breaker type. Wave period also seems to have considerable influence on the range of up-rush and down-rush, which in turn influences the transport rate in the swash zone. The KAMPHUIS-91 formula under-predicted the spilling and plunging cases by 17% and 24%, respectively. The consistent under-prediction, if confirmed with more data, can be resolved by adjusting the empirical coefficient.

Different comprehension and parameterization were used in the KRAUS *et al.* (1988) formula. The threshold value R_c of 3.9 m^3/s, which was determined from an Atlantic Ocean surf zone, is too large for application in the laboratory beach. Since the main purpose of the present comparison is to examine the consistency of predictions for different breaker types, and also because little is known about the factors controlling R_c, this parameter is ignored here. The recommended K_d value of 2.7 is still used. The longshore discharge was measured directly in the LSTF through the circulation pumps (HAMILTON and EBERSOLE, 2001). It was not necessary in this case to use Equation 8 to calculate the total discharge. Predictions from the KRAUS-88 formula are also compared in Table 3. The predicted value compared well with the spilling case, but under-predicted the plunging case by 55%. As dis-

cussed in KRAUS *et al.* (1988), the coefficient K_d is related to sediment suspension. Based on discussions in the previous sections, sediment suspension in the vicinity of the spilling and plunging breaker lines was substantially different. The inconsistency in the prediction using the method of KRAUS *et al.* (1988) was caused by neglecting the different magnitudes of sediment suspension and using a constant K_d value. The K_d value for plunging breakers should be greater due to the much more active sediment suspension. Similar to the situation encountered by using the KRAUS-88 formula, the inconsistency of the CERC formula and KAMPHUIS-86 formula probably arose for a similar reason. The significantly improved consistency of the KAMPHUIS-91 formula was likely caused by the incorporation of wave period, which has significant influence on the breaker type and swash transport.

CONCLUSIONS

In the vicinity of the breaker line, sediment suspension was much more active under the plunging breakers than under spilling breakers. High in the water column, at elevations greater than 5 cm from the bed, suspended sediment concentration was more than one order of magnitude greater under the plunging breakers than under spilling breakers of similar breaking wave height. The greater sediment suspension was apparently related to the much more turbulent plunging-type breaking, as also reflected in a steep rate of wave-height decay immediately following the breaking of the plunging waves. This substantial difference was not measured in the mid-surf zone dominated by surf-bore motions, where slightly greater suspended sediment concentrations were measured under the spilling breakers. The surf-bore motions seemed to be independent of the breaker type.

Cross-shore distribution of the depth-averaged longshore current, as well as the vertical profile of the current, was not significantly influenced by breaker type. Similar vertical profile and depth-averaged longshore current were measured during the spilling and plunging breakers. These were probably controlled by the similar breaker height and angle, and the cross-shore pattern of wave decay. During both the spilling and plunging cases, the peak longshore current was measured just seaward of the swash zone at the landward-most current meter 1.1 m from the still-water shoreline. Longshore current in the swash zone could not be measured due to the shallow water with 100% depth variation. Visual observations of dye movement indicated that longshore current in the swash zone was of the similar magnitude as that measured at the landward-most current meter. A subtle secondary peak was evident just shoreward of the main breaker line in both cases.

Influenced by the different suspended-sediment concentrations, the total rate and cross-shore distribution of longshore sediment transport were significantly different during the plunging and spilling cases. Nearly 170% more longshore sediment transport was measured for the plunging-breaker case than for the spilling-breaker case, although the plunging-breaker height was only 4% higher than the spilling-breaker height. The cross-shore distribution of longshore sediment transport was far from being uniform. During the spilling-breaker case, peak longshore transport was measured in the swash zone. During the plunging-breaker case, two transport peaks were measured, one in the swash zone and one in the vicinity of the breaker line. Substantial amounts of longshore sediment transport were measured in the swash zone during both cases. Interestingly, in the mid-surf zone dominated by surf-bore motions, the measured transport rates were rather similar for both the spilling and plunging cases. In other words, the much greater rate of total longshore transport measured for the plunging case than for the spilling case was mainly contributed by the much more active sediment suspension and transport in the breaker zone and more transport in the wider and more active swash zone.

The commonly used CERC formula predicted inconsistent total longshore sediment transport rate under the spilling and plunging breakers. It may be necessary to adjust the empirical K_l for different breaker types. By including wave period, which has significant influence on breaker type, the KAMPHUIS-91 formula produced consistent predictions for both the spilling and plunging cases, although underestimated by about 20%. Results from the present study suggest that breaker type has a significant influence on the total rate of longshore sediment transport and its cross-shore distribution pattern. Parameterization of predictive formulas should include factors that reflect the breaker type.

In terms of breaker height and angle, the two most commonly used parameters in predicting longshore sediment transport rate in the surf zone, the present laboratory data are directly comparable to some of the field measurements under low-wave energy conditions. Although not directly examined in this paper, valuable knowledge could be learned through a comparison of laboratory and field data.

ACKNOWLEDGMENTS

David Hamilton, William Halford, David Daily, and Tim Nisley provided technical support for this study. We thank Carl Miller and Reggie Beach for providing the FOBS sensors. The paper benefited greatly from the constructive reviews by Dr. Mark Schmeeckle, Dr. Jane Smith, and an anonymous reviewer. Ping Wang is jointly funded by the U.S Army Engineer Research and Development Center and the Louisiana Sea Grant College Program. Permission to publish this paper was granted by the Headquarters, U.S. Army Corps of Engineers.

LITERATURE CITED

BATTJES, J.A., 1974. Surf similarity. *Proceedings of 14th International Conference on Coastal Engineering,* New York: ASCE press, pp. 466–479.

BODGE, K.R., 1986. Short term impoundment of longshore sediment transport. Ph.D. Dissertation, University of Florida, 345p.

BODGE, K.R. and DEAN, R.G., 1987. Short-term impoundment of longshore transport. *Proceedings of Coastal Sediments '87,* New York: ASCE press, pp. 468–483.

BODGE, K. R. and KRAUS, N. C., 1991. Critical examination of longshore transport rate magnitude. *Proceedings Coastal Sediments '91,* New York: ASCE Press, pp. 139–155.

BOSMAN, J., 1982. Concentration measurements under oscillatory motion. Delft Hydraulics, *Report MI695-II,* Deft, the Netherlands.

BOUWS, E.H.; ROSENTHAL, G.W., and VINCENT, C.L., 1985. Similarity of the wind wave spectral in finite water depth, 1: spectral form. *Journal of Geophysical Research,* 90, 975–986.

BRUUN, P., 1954. Coast erosion and the development of beach profiles. *Technical Memorandum No. 44,* Beach Erosion Board.

CERC, 1984. *Shore Protection Manual.* U.S. Army Corps of Engineers, Coastal Engineering Research Center, U.S. Government Printing Office, Washington, D.C.

DALLY, W.R., 1990. Random breaking waves: a closed-form solution for planar beaches. *Coastal Engineering,* 14, 233–263.

DALLY, W.R., 1992. Random breaking waves: field verification of a wave-by-wave algorithm for engineering application. *Coastal Engineering,* 16, 369–397.

DALLY, W.R.; DEAN, R.G., and DALRYMPLE, R.A., 1985. Wave height variation across beaches of arbitrary profile. *Journal of Geophysical Research,* 90, 11,917–11,927.

DAVIS, R.A.; WANG, P., and SILVERMAN, B.R., 2000. Comparison of the performance of three adjacent and differently constructed beach nourishment projects on the Gulf peninsula of Florida. *Journal of Coastal Research,* 16, 396–408.

DEAN, R.G., 1973. Heuristic models of sand transport in the surf zone. *Proceedings of Conference on Engineering Dynamics in the Surf Zone,* pp. 208–214.

DEAN, R.G., 1977. Equilibrium beach profiles: U.S. Atlantic and Gulf coasts. *Ocean Engineering Report No. 12,* Department of Civil Engineering, University of Delaware, Newark, Delaware.

DEAN, R.G., 1989. Measuring longshore sediment transport with traps. *In:* SEYMOUR, R.J. (ed.), *Nearshore Sediment Transport,* New York: Plenum Press, pp. 313–337.

DEAN, R.G., 1991. Equilibrium beach profiles: characteristics and applications. *Journal of Coastal Research,* 7, 53–84.

DEAN, R.G. and DALRYMPLE, R.A., 1991. *Water Wave Mechanics for Engineers and Scientists.* Singapore: World Scientific, 353p.

DEIGAARD, R.; FREDSOE, J., and HEDEGAARD, I.B., 1986. Mathematical model for littoral drift. *Journal of Waterway, Port, Coastal and Ocean Engineering,* ASCE, 112(3), 351–369.

FOWLER, J.E.; ROSATI, J.D.; HAMILTON, D.G., and SMITH, J.M., 1995. Development of a large-scale laboratory facility for longshore sediment transport research. *The CERCular, CERC-95–2,* U.S. Army Engineer Waterways Experiment Station, Vicksburg, MS.

GALVIN, C.J., 1968. Breaker type classifications of three laboratory beaches. *Journal of Geophysical Research,* 73, 3651–3659.

HALLERMEIER, R.J., 1981. Terminal settling velocity of commonly occurring sand grains. *Sedimentology,* 28, 859–865.

HAMILTON, D.G.; EBERSOLE, B.A.; SMITH, E.R., and WANG, P., 2001. Development of a large-scale laboratory facility for sediment transport research. *Technical Report* ERDC/CHL-TR-01-22, U.S. Army Engineer Research and Development Center, Vicksburg, Mississippi.

HAMILTON, D.G. and EBERSOLE, B.A., 2001. Establishing uniform longshore currents in a large-scale laboratory facility. *Coastal Engineering,* 42, 199–218.

INMAN, D.L.; ZAMPOL, J.A.; WHITE, T.E.; HANES, B.W.; WALDORF, B.W., and KASTENS, K.A., 1981. Field measurements of sand motion in the surf zone. *Proceedings of 17th International Conference on Coastal Engineering,* New York: ASCE press, pp. 1215–1234.

KAMINSKY, G. and KRAUS, N. C., 1994. Evaluation of depth-limited breaking wave criteria. *Proceedings of Ocean Wave Measurement and Analysis,* New York: ASCE Press, pp. 180–193.

KAMPHUIS, J.W., 1991a. Alongshore sediment transport rate. *Journal of Waterway, Port, Coastal and Ocean Engineering,* ASCE, 117(6), 624–641.

KAMPHUIS, J.W., 1991b. Wave transformation. *Coastal Engineering,* 15, 173–184.

KAMPHUIS, J.W., 1991c. Incipient wave breaking. *Coastal Engineering,* 15, 185–203.

KAMPHUIS, J.W.; DAVIES, M.H.; NAIRN, R.B., and SAYAO, O.J., 1986. Calculation of littoral sand transport rate. *Coastal Engineering,* 10, 1–21.

KANA, T.W., 1979. Suspended sediment in breaking waves. *Technical Report No. 18-CRD,* University of South Carolina, Department of Geology, Columbia, South Carolina. 153p.

KANA, T.W. and WARD, L.G., 1980. Suspended sediment load during storm and post storm conditions. *Proceedings of 17th International Conference on Coastal Engineering,* New York: ASCE, pp. 1159–1175.

KOMAR, P.D., 1998. *Beach Processes and Sedimentation.* New Jersey: Prentice-Hall, 544p.

KOMAR, P.D. and INMAN, D.L., 1970. Longshore sand transport on beaches. *Journal of Geophysical Research,* 75(30), 5514–5527.

KRAUS, N.C. and SASAKI, T.O., 1979. Influence of wave angle and lateral mixing on the longshore current. *Marine Science Communications,* 5(2), 91–126.

KRAUS, N.C.; ISOBE, M.; IGARASHI, H.; SASAKI, T.O., and HORIKAWA, K., 1982. Field experiments on longshore transport in the surf zone. *Proceedings of 18th International Conference on Coastal Engineering,* New York: ASCE press, pp. 969–988.

KRAUS, N.C. and DEAN, J.L., 1987. Longshore sediment transport rate distributions measured by trap. *Proceedings of Coastal Sediments'87,* New York: ASCE press, pp. 818–896.

KRAUS, N.C.; GINGERICH, K.J., and ROSATI, J.D., 1988. Toward an improved empirical formula for longshore sand transport. *Proceedings of 21st Coastal Engineering Conference,* New York: ASCE press, pp. 1183–1196.

KRAUS, N.C. and LARSON, M., 1991. NMLONG: Numerical model for simulating the longshore current—Report 1: model development and tests. *Technical Report DRP-91-1,* U.S. Army Engineer Waterways Experiment Station, Vicksburg, Mississippi.

LONGUET-HIGGINS, M.S., 1970. Longshore currents generated by obliquely incident waves, 1 and 2. *Journal of Geophysical Research,* 75, 6778–6810.

MILLER, H.C., 1998. Comparison of storm longshore transport rates to predictions. *Proceedings of 26th International Conference on Coastal Engineering,* New York: ASCE Press, pp. 2953–2967.

MILLER, H.C., 1999. Field measurements of longshore sediment transport during storms. *Coastal Engineering,* 36, 301–321.

NIELSEN, P., 1979. Some basic concepts of wave sediment transport. *Serial Paper 20,* Institute of Hydrodynamic and Hydraulic Engineering, Technical University of Denmark, 160pp.

NIELSEN, P., 1984. Field measurements of time-averaged suspended sediment concentrations under waves. *Coastal Engineering,* 8, 51–72.

NIELSEN, P., 1992. *Coastal Bottom Boundary Layers and Sediment Transport.* Singapore: World Scientific, p. 109–110.

NORDSTROM, K.F., 1992. *Estuarine Beaches.* Amsterdam: Elsevier Applied Science, 225 pp.

PATRICK, D.A. and WIEGEL, R.L., 1957. Amphibian tractors in the surf. *Proceedings of the First Conference on Ships and Waves,* The Engineering Foundation Council on Wave Research and the American Society of Naval Architects and Marine Engineers, 397–422.

SCHOONEES, J.S. and THERON, A.K., 1993. Review of the field database for longshore sediment transport. *Coastal Engineering,* 19, 1–25.

SCHOONEES, J.S. and THERON, A.K., 1994. Accuracy and applicability of the SPM longshore transport formula. *Proceedings of the 24th Coastal Engineering Conference,* New York: ASCE Press, pp. 2595–2609.

SLINN, D.N.; ALLEN, J.S., and HOLMAN, R.A., 2000. Alongshore currents over variable beach topography. *Journal of Geophysical Research,* 105, 16,971–16,998.

SMITH, E.R. and KRAUS, N.C., 1991. Laboratory study of wave-breaking over bars and artificial reefs. *Journal of Waterway, Port, Coastal and Ocean Engineering,* ASCE, 117, 307–325.

SMITH, J.M.; LARSON, M., and KRAUS, N.C., 1993. Longshore current on a barred beach: Field measurements and calculations. *Journal of Geophysical Research,* 98, 22,717–22,731.

SVENDSEN, I.A., 1984a. Wave heights and set-up in a surf zone. *Coastal Engineering,* 8, 303–329.

SVENDSEN, I.A., 1984b. Mass flux and undertow in a surf zone. *Coastal Engineering,* 8, 347–365.

SVENDSEN, I.A. and LORENZ, P., 1989. Velocities in combined undertow and longshore currents. *Coastal Engineering,* 13, 55–79.

THORNTON, E.B. and GUZA, R.T., 1983. Transformation of wave height distribution. *Journal of Geophysical Research,* 88, 5925–5938.

TING, F.C.K. and KIRBY, J.T., 1994. Observation of undertow and turbulence in a laboratory surf zone. *Coastal Engineering,* 24, 51–80.

TING, F.C.K. and KIRBY, J.T., 1995. Dynamics of surf-zone turbulence in a strong plunging breaker. *Coastal Engineering,* 24, 177–204.

TING, F.C.K. and KIRBY, J.T., 1996. Dynamics of surf-zone turbulence in a spilling breaker. *Coastal Engineering,* 27, 131–160.

VAN RIJN, L.C., 1993. *Principles of sediment transport in rivers, estuaries and coastal seas.* The Netherlands: Aqua Publications.

VAN RIJN, L.C. and KROON, A., 1992. Sediment transport by currents and waves. *Proceedings of 23rd International Conference on Coastal Engineering,* New York: ASCE Press, pp. 2613–2628.

VISSER, P.J., 1991. Laboratory measurements of uniform longshore currents. *Coastal Engineering,* 15, 563–593.

WANG, P., 1998. Longshore sediment flux in the water column and across the surf zone. *Journal of Waterway, Port, Coastal & Ocean Engineering,* ASCE, 124, 108–117.

WANG, P.; KRAUS, N.C., and DAVIS, R.A., JR., 1998a. Total rate of longshore sediment transport in the surf zone: field measurements and empirical predictions. *Journal of Coastal Research,* 14(1), 269–283.

WANG, P.; DAVIS, R.A., JR., and KRAUS, N.C., 1998b. Cross-shore distribution of sediment textures under breaking waves. *Journal of Sedimentary Research,* 68, 497–506.

WANG, P. and KRAUS, N.C., 1999. Longshore sediment transport rate measured by short-term impoundment. *Journal of Waterway, Port, Coastal and Ocean Engineering,* ASCE, 125, 118–126.

WANG, P.; EBERSOLE, B.A.; SMITH, E.R., and JOHNSON, B., in review. Temporal and spatial variations of surf-zone currents and suspended-sediment concentration: a case study at the large-scale sediment transport facility, in review at *Coastal Engineering.*

ZAMPOL, J.A. and INMAN, D.L., 1989. Discrete measurement of suspended sediment. *In:* SEYMOUR, R.J. (ed.), *Nearshore Sediment Transport.* New York: Plenum Press, pp. 257–285.